Basin Research (2004) **16**, 279–296, doi: 10.1111/j.1365-2117.2004.00233.x

Timing of depth-dependent lithosphere stretching on the S. Lofoten rifted margin offshore mid-Norway: pre-breakup or post-breakup?

N. J. Kusznir,* R. Hunsdale†[1] and A. M. Roberts‡

*Department of Earth & Ocean Sciences, University of Liverpool, Liverpool, UK
†Technology Division, Statoil ASA, Forushagen, 4035 Stavanger, Norway
‡Badley Geoscience Ltd, Hundleby, Spilsby, Lincolnshire, UK

ABSTRACT

Depth-dependent stretching, in which whole-crustal and whole-lithosphere extension is significantly greater than upper-crustal extension, has been observed at both non-volcanic and volcanic rifted continental margins. A key question is whether depth-dependent stretching occurs during pre-breakup rifting or during sea-floor spreading initiation and early sea-floor spreading. Analysis of post-breakup thermal subsidence and upper-crustal faulting show that depth-dependent lithosphere stretching occurs on the outer part of the Norwegian volcanic rifted margin. For the southern Lofoten margin, large breakup lithosphere β stretching factors approaching infinity are required within 100 km of the continent–ocean boundary to restore Lower Eocene sediments and flood basalt surfaces ($\sim$54 Ma) to interpreted sub-aerial depositional environments at sea level as indicated by well data. For the same region, the upper crust shows no significant Palaeocene and Late Cretaceous faulting preceding breakup with upper-crustal β stretching factors < 1.05. Further north on the Lofoten margin, reverse modelling of post-breakup subsidence with a β stretching factor of infinity predicts palaeo-bathymetries of $\sim$1500 m to the west of the Utrøst Ridge and fails to restore Lower Eocene sediments and flood basalt tops to sea level at $\sim$54 Ma. If these horizons were deposited in a sub-aerial depositional environment, as indicated by well data to the south, an additional subsidence event younger than 54 Ma is required compatible with lower-crustal thinning during sea-floor spreading initiation. For the northern Vøring margin, breakup lithosphere β stretching factors of $\sim$2.5 are required to restore Lower Eocene sediments and basalts to sea level at deposition, while Palaeocene and Late Cretaceous upper-crustal β stretching factors for the same region are < 1.1. The absence of significant Palaeocene and late Cretaceous extension on the southern Lofoten and northern Vøring margins prior to continental breakup supports the hypothesis that depth-dependent stretching of rifted margin lithosphere occurs during sea-floor spreading initiation or early sea-floor spreading rather than during pre-breakup rifting.

INTRODUCTION

Depth-dependent stretching of continental lithosphere has been observed at many rifted continental margins (Roberts *et al*., 1997; Driscoll & Karner, 1998; Davis & Kusznir, 2004). Stretching estimates, independently determined from upper-crustal faulting, whole-crustal thinning and post-rift lithosphere thermal subsidence (Fig. 1a), show that extension increases with depth within $\sim$150 km of the continent–ocean boundary (COB) such that whole-crustal and whole-lithosphere extension are significantly greater than upper-crustal extension. Further towards the continent, stretching and thinning estimates of the upper crust, whole crust and lithosphere converge as the β stretching factors decrease. Total continental margin extension may be determined by laterally integrating the thinning factor $(1 - 1/\beta)$ across the margin (Davis & Kusznir, 2004). Margin extension is summarised in Fig. 1b for Goban Spur margin offshore UK, South China Sea margin, Exmouth Plateau margin offshore W Australia, Vøring Basin margin offshore Norway and Vulcan Basin margin offshore NW Australia (Roberts *et al*., 1997; Driscoll & Karner, 1998; Baxter *et al*., 1999; Davis & Kusznir, 2004). Extension of the whole crust and lithosphere exceeds that of the upper crust in all cases and occurs at both volcanic and non-volcanic margins. Depth-dependent lithosphere stretching appears to be a fundamental property of all rifted continental margins and provides an important constraint in determining the geodynamic processes responsible for rifted margin formation. An important

Correspondence: N. J. Kusznir, Department of Earth & Ocean Sciences, University of Liverpool, Liverpool L69 3BX, UK. E-mail: N.Kusznir@liverpool.ac.uk
[1] Previously at Phillips Petroleum Company, Tananger, Norway.

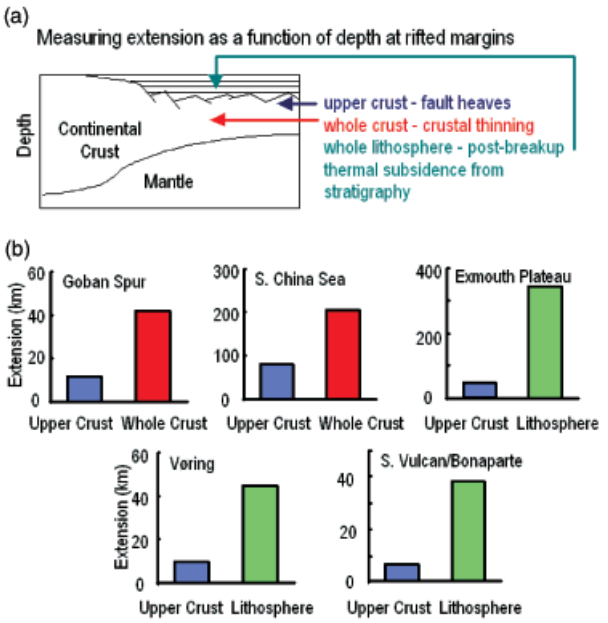

Fig. 1. (a) Extension and thinning at rifted continental margins can be measured at the levels of the upper crust, the whole crust and the lithosphere using 3 distinct data sets and methodologies. (b) The Goban Spur, S. China Sea, Exmouth Plateau, Vøring and Vulcan Basin margins show depth-dependent lithosphere stretching; whole-crustal and whole-lithosphere extension are significantly greater than upper-crustal extension.

question is whether depth-dependent stretching occurs during pre-breakup rifting or during early sea-floor spreading. In order to answer this question good stratigraphic resolution at and immediately preceding continental breakup is required. The southern Lofoten and northern Vøring rifted continental margins offshore Norway satisfy this requirement and provide an excellent natural laboratory to answer this question.

The objectives of this study are to determine the magnitude and timing of lithosphere stretching for both the whole lithosphere and the upper crust for the southern Lofoten and northern Vøring segments of the Norwegian rifted continental margin. Stretching and thinning have been determined for the whole lithosphere using post-breakup thermal subsidence, while upper-crustal stretching has been estimated from upper-crustal faulting. Because volcanic addition has modified crustal thickness for the Vøring and Lofoten continental margin (Mjelde *et al.*, 1993), no attempt has been made in this study to estimate stretching factors for the whole crust as these estimates are likely to be inaccurate.

In order to determine the magnitude and timing of southern Lofoten and northern Vøring rifted margin stretching and its distribution with depth, stratigraphic modelling has been applied to depth-converted cross-sections of margin stratigraphy. Flexural backstripping, decompaction and reverse post-rift subsidence modelling (Kusznir *et al.*, 1994; Roberts *et al.*, 1998) have been used to produce a series of reconstructed cross-sections whose palaeo-bathymetry depends on the magnitude of the lithosphere stretching factor (McKenzie, 1978) used in the reverse thermal subsidence model. Restored cross-sections are tested against observed palaeo-bathymetry so permitting the magnitude of lithosphere stretching to be determined. In addition, forward syn-rift modelling using the flexural cantilever model (Kusznir *et al.*, 1991) has been used to provide estimates of fault extension (independent from that derived by flexural backstripping and reverse post-rift modelling).

The stratigraphic analysis using structural and stratigraphic modelling has been divided into three components in order that the timing of whole-lithosphere and upper-crustal stretching may be determined with respect to the time of continental breakup:

(1) analysis of end Palaeocene–early Eocene extension associated with continental breakup and the start of sea-floor spreading.
(2) analysis of Palaeocene extension prior to continental breakup.
(3) analysis of Late Cretaceous extension.

Line locations are shown superimposed on maps showing the pre-breakup Atlantic margin restoration at 55 Ma (Fig. 2a) and present day margin location (Fig. 2b). The geological interpretation of the depth-converted cross-sections for lines 1, 2 and 3 used in this study are shown in Fig. 3. Comparisons with bathymetry and magnetic anomaly data (Mosar *et al.*, 2002; Sigmond, 2002) and earlier geophysical work (Mjelde *et al.*, 1993; Tsikalas *et al.*, 2001) suggest that line 3 extends westwards $\sim$50 km onto oceanic crust, while lines 1 and 2 extend westwards to the COB. Not all stratigraphic horizons were identifiable on all of the profiles; in particular, the top Paleogene reflector is absent on lines 1 and 3. Also, the basalts as mapped on the marginal high are restricted to the areas west of the Utrøst Ridge (Fig. 3). Extension of horizons under the thick basalt in the west is somewhat subjective and pre-basalt picks are extended laterally as a wedge that thins gently westward onto a basement high. Sediment thickness varies between 1.5 and 2.5 km. This is in keeping with estimates of pre-basalt sedimentary thicknesses determined from seismic refraction and potential field data in this area (Mjelde *et al.*, 1993; Tsikalas *et al.*, 2001).

The lithological units, and their stratigraphic ages and compaction parameters (surface porosity, compaction constant and matrix density), selected for the flexural backstripping and reverse post-rift modelling are summarised in Table 1. For all sedimentary units composition is determined from a regional well database. Matrix densities for the basalts are taken from descriptions of ODP site 642 (Eldholm *et al.*, 1989), supplemented with data from further south and west within the North Atlantic Igneous Province. ODP 642 penetrates 914 m of mixed lava flows and volcanoclastics whose matrix density varies from 1.95 to 3.05 g cm^{-3} with a mean density of 2.66 g cm^{-3} (Eldholm *et al.*, 1989). Geophysical evidence from the margin (Mjelde *et al.*, 1993, 1998) suggests that the basalt pile is of the order of 1–3 km thick. Although ODP 642 encounters a

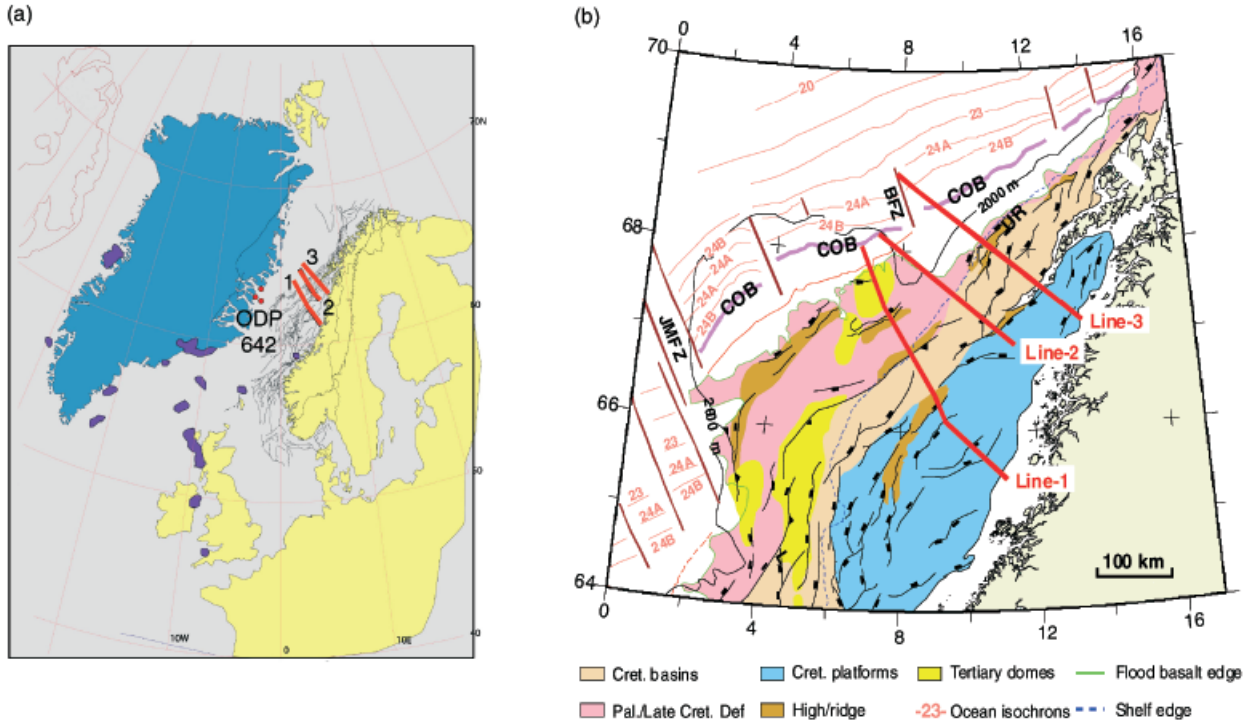

Fig. 2. The location of lines 1, 2 and 3 on the southern Lofoten and northern Vøring segments of the Mid-Norwegian continental margin used in this study superimposed on: (a) a plate reconstruction at 54 Ma (after Eide, 2002) and on: (b) a present day map showing the location of the COB and major structural elements (after Tsikalas *et al.*, 2001). UR = Utrøst Ridge, COB = continent–ocean boundary, BFZ = Bivrøst Fracture Zone, JMFZ = Jan Mayen Fracture Zone.

mixed volcanic sequence, the likelihood is that along the margin, just as observed farther south, the nature of the volcanic pile changes to more massive flows. To account for this a matrix density range of 2.7–2.85 g cm^{-3} is used for basalt.

BACKGROUND

The Lofoten margin encompasses an approximately 400 km section of the North Atlantic volcanic passive margin that links the rifted Mid-Norwegian margin with the transform margin of the southwest Barents Sea (Sigmond *et al.*, 2002). In this study, profiles from the southern sector of the Lofoten volcanic margin and the northernmost Vøring Basin (Fig. 3) are examined. A northwest–southeast trending fracture zone, the Bivrøst Lineament, is coincident with a prominent oceanic transform fault, the Bivrøst Fracture Zone, which separates the Vøring and Lofoten basins. Although no large fault offsets can be demonstrated on seismic lines running perpendicular to this fracture zone, seismic data shows evidence of marked stratigraphic thickness variations across the zone suggesting that at least through the Late Cretaceous and into the Early Tertiary, this zone acted as a hinge, controlling sediment accommodation space and palaeogeography. Line 1 lies to the south of the Bivrøst Lineament, line 2 crosses the Bivrøst Lineament, and line 3 lies to the north of the Bivrøst Fracture Zone and Lineament (Tsikalas *et al.*, 2001). From south to north the margin is characterised by a gradually narrowing continental shelf that slopes steeply towards the ocean basin. Water depths also increase from around 1800 m at the western end of line 1, to 2300 m at the end of line 2, to 3200 m at the end of line 3 (Figs 2 and 3).

Over recent years, ConocoPhillips Norway have undertaken an integrated regional mapping program with the aim of developing a tectono-stratigraphic framework for the Norwegian Sea. The integration of well data with the regional seismic database led to a series of regional marker horizons, some of which relate to establishing key stages in the tectonic evolution of the basin. Within the context of the work presented here, the key surfaces exist in the lower part of the Cenozoic and are referred to as the top Tare, top Basalt and Base Basalt in Table 1. The importance of age, palaeo-bathymetry, palaeo-topography and environment of deposition for these surfaces is discussed later in this section. Cretaceous and Triassic surfaces referred to in Table 1 are presented in the nomenclature of the tectono-stratigraphic scheme of ConocoPhillips with absolute ages given for reference. The stratigraphic ages are based of the time scales of Gradstein *et al.* (1994) for the Mesozoic, Berggren *et al.* (1995) for the Cenozoic and the magnetostratigraphy of Cande & Kent (1992). Lithostratigraphic correlations were based on the work of Dalland *et al.* (1988).

Like the rest of the NW European continental margin, the Lofoten margin has a prolonged history of intermittent extension from Devonian post-orogenic collapse, through to the formation of the continental margin at the

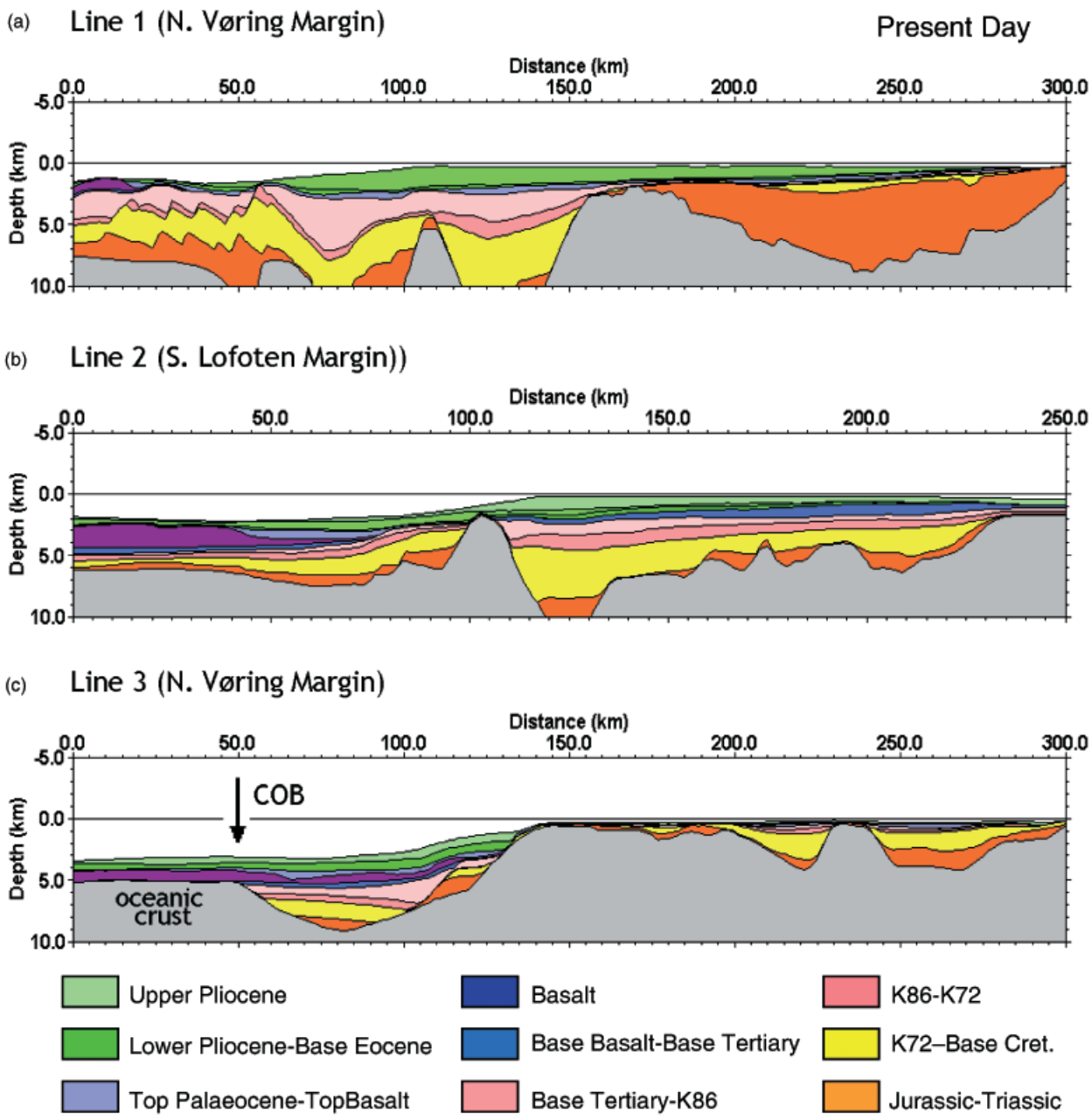

Fig. 3. Interpretations of depth converted cross-sections for lines 1, 2 and 3 across the southern Lofoten margin and northern Vøring rifted continental margin used in this study. Horizon ages are given in Table 1. Line 3 extends 50 km onto oceanic crust to the NW (Mosar *et al.*, 2002). Line 2 crosses the Bivrøst Lineament.

start of the Eocene (Eldholm *et al.*, 1989; Blystad *et al.*, 1995; Eldholm *et al.*, 1995; Lundin & Doré 1997; Doré *et al.*, 1999; Roberts *et al.*, 1999; Brekke, 2000; Skogseid *et al.*, 2000). Most authors agree on the main rift phases being Early Triassic, Middle to Late Jurassic, Early Cretaceous and Late Cretaceous to Palaeocene, the latter ultimately leading to continental margin formation (Talwani & Eldholm, 1972, 1977; Eldholm *et al.*, 1989; Lundin & Doré, 1997; Skogseid *et al.*, 2000). Doré *et al.* (1999) and Lundin & Doré (1997) have also suggested that significant rifting occurred during the middle part of the Cretaceous. Seismic evidence from the Møre, Vøring and Lofoten Basins and a previous structural modelling campaign undertaken by ConocoPhillips in the former two basins supports the notion of significant middle Cretaceous rifting.

For simplicity, most authors define two main phases in the failure history of the Mid-Norwegian basins. The first is the Middle Jurassic to Early Cretaceous rifting responsible for the distribution of Upper Jurassic reservoirs and the formation of structurally controlled traps around the Halten-Dønna Terrace systems flanking the Triassic Trøndelag Platform. The second is the Late Cretaceous to Early Tertiary rifting that is concentrated oceanward of the Jurassic terrace systems in the deepwater Vøring Basin. The latter rifting phase is interpreted to have ultimately led to continental separation in the early Eocene. Both rift

Table 1. Stratigraphic units, base ages, and compaction parameters used in reverse post-rift modelling.

Horizon at base of stratigraphic unit	Age of base of lithological unit (ma)	Initial porosity (%)	Compaction constant (km^{-1})	Matrix density ($gm\ cm^{-3}$)
Seabed	0	–	–	–
Base quaternary	1.8	59	0.44	2.7
Base upper Pliocene	2.6	59	0.44	2.7
Top paleogene	24	60	0.46	2.71
Top tare	54	61	0.47	2.71
Top basalt	54.1	61	0.47	2.71
Base basalt	58	0	–	2.85
Base tertiary	65	62	0.49	2.72
K86	67	54	0.53	2.72
K72	81.5	61	0.48	2.71
K64	87	58	0.43	2.7
K54	93.5	62	0.51	2.71
K20	117	58	0.43	2.71
Base cretaceous unconformity	142	62	0.49	2.71
Tr50	205	61	0.48	2.71
Tr10	231	56	0.39	2.68
Top basement	250	56	0.39	2.68

phases are effectively finite rift periods extending over periods of approximately 50 Myr, 175–125 Ma and 100–54 Ma, respectively. Although normal faulting within these basins is widely observed, few quantitative estimates of basin extension have been presented (Roberts *et al.*, 1997; Skogseid *et al.*, 2000).

The pattern seen in the Vøring Basin of a western Cretaceous basin lying outboard of a Jurassic–Triassic rift system is repeated on the Lofoten margin. The defining fault zone lies along the western flank of the Utrøst Ridge (Fig. 2). West of the Utrøst Ridge most of the Mesozoic section is hidden under lower Tertiary trap lavas; to the east the Tertiary and Mesozoic section is gradually eroded out northward under a marked unconformity thought to be related to the distribution of ground ice during the Pleistocene glaciations (Riis & Fjeldskaar, 1992). Despite this unconformity, the remaining Lower Tertiary section on the Lofoten margin suggests that the Upper Palaeocene and Lower Eocene sections plunge to the southwest along the Ribban and Vestfjord basins, thickening towards the Bivrøst Lineament. Due to the northward-deepening erosion level beneath the Pleistocene unconformity, the Paleogene section, for the most part, is missing in the area of line 3.

In undertaking this modelling, some important assumptions were made relating both to the timing of continental separation and the nature of the palaeobathymetry/topography along the western part of the section in the area close to the line of breakup. The age of breakup is estimated from the occurrence of the first definitive magnetic anomaly, Anomaly 24B (Skogseid *et al.*, 2000; Sigmond, 2002; Tsikalas, *et al.*, 2002). Based on the timescale of Cande & Kent (1992) this anomaly has an age of 53.9 Ma and can be described as earliest Eocene. We note some debate regarding the exact age of the Palaeocene–Eocene boundary (Prince, pers. comm.), however discussion of this is beyond the scope of this paper. Tsikalas *et al.* (2002) have suggested that early N Atlantic opening may have commenced as early as 54.6 Ma. For modelling purposes we use 54 Ma as the time of continental breakup, and as a proxy age for the top Tare formation reflector. The top Tare as mapped seismically is not coincident with the top of the Tare Formation; rather, the seismic pick follows a prominent reflector sequence that ties to the top of a tuffaceous sequence in many wells. Previous work suggests that this is a regional, mappable event that that is somewhat diachronous in nature (Dalland *et al.*, 1988; Berggren *et al.*, 1995). At wells in the north Vøring Basin, the top Tare tuff sequence has been correlated to the Palaeocene–Eocene boundary (6607/5–2, Ren *et al.*, 2003) supporting the date used here. In a broader context the top Tare is time-equivalent to the top Balder tuff sequence from the North Sea and Faroes-Shetland regions. In these latter areas, an age of 54 Ma is also used for the top of the tuff sequence (e.g. Nadin & Kusznir, 1995).

The age of the top of the top Basalt reflector has not been definitively established on the Norwegian Sea marginal highs and in this study we use a proxy age of 54.1 Ma, placing the top Basalt reflector just older than top Tare (Table 1). One date on an extrusive rock exists from the Vøring margin at ODP 642, but this is not from the top of the sequence and gives an age of 55 Ma (Sinton *et al.*, 1998). On a pre-break up reconstruction at 55 Ma (Fig. 2a) the position of ODP site 642 can be seen in relation to radiometric data points in the Traill Ø–Hold with Hope area of East Greenland (Price *et al.*, 1997; Upton *et al.*, 1995). Data from here gives complementary ages placing the main igneous pulse in the 58–54 Ma range of the North Atlantic Igneous Province (Saunders *et al.*, 1997). This is comparable with a more statistically significant database from the southern part of the North Atlantic Igneous

Province (Eide, 2003, pers. comm.). Based on data from the North Atlantic, ages of 54.1 and 58 Ma are considered reasonable for the top and bottom of the basalt pile.

The second major assumption to this modelling work is that in the Early Eocene sediments of the Tare Formation and at least a part of the basalt pile were deposited or extruded in emergent or relatively shallow-water conditions. There is no well control on this part of the Lofoten Margin outboard of the Utrøst Ridge. On the volcanic marginal high of the Norwegian Sea the only wells that test rocks of Lower Eocene age, directly overlying basalt are south of the Bivrøst Lineament in the outer Vøring Basin (Talwani & Eldholm, 1972; Eldholm *et al*., 1989). Wells in this area indicate that at least parts of the margin were emergent and that both basaltic and sialic, possibly sedimentary material, were being eroded (Talwani & Eldholm, 1972; Caston, 1976). Perhaps the most compelling evidence for emergence comes from ODP well 642 where 914 m of interbedded basalt flows and volcanoclastics are encountered; according to Eldholm *et al*. (1989) 'the entire series was deposited under terrestrial conditions'. Further north at DSDP sites 338 and 343 clastic sediments of Tare age are marine in nature. However, Caston (1976) suggests that the Lower Eocene sediments contain clasts of material indicating that nearby, emergent basalt highs were being actively eroded. Indeed seismic and stratigraphic evidences from DSDP site 342 (Talwani & Eldholm, 1972) show that the basalts are onlapped by Tertiary sediments and that some parts of the high may have been emergent into the Early Miocene.

METHODOLOGY OF REVERSE POST-RIFT MODELLING AND FORWARD SYN-RIFT MODELLING

Reverse post-rift modelling

Thermal subsidence, sediment loading and compaction, in addition to sediment supply, control post-breakup subsidence on rifted margins. Thermal subsidence arises from the cooling of stretched continental lithosphere (McKenzie, 1978) and the recently formed oceanic lithosphere. The isostatic response of the lithosphere to cooling and sediment loading is regionally distributed by the flexural strength of the lithosphere. Post-breakup subsidence and palaeo-bathymetry may be reverse modelled using flexural backstripping and reverse post-rift modelling (Kusznir, *et al*., 1994; Roberts, *et al*., 1997; Roberts *et al*., 1998). Flexural backstripping and reverse post-rift modelling consist of the following processes:

(1) Removal of the current topmost stratigraphic unit.
(2) Decompaction of the remaining deeper lithologies.
(3) Computation of the net removed mass of sediment matrix and water as a consequence of the removal of the topmost current layer and the resulting decompaction of deeper lithologies.
(4) Computation of incremental post-rift thermal subsidence corresponding to the ages of removed stratigraphic units using knowledge of the β stretching factor (McKenzie 1978) and rift age.
(5) Computation of the flexural isostatic response to removed mass of sediment matrix and water, and thermal subsidence.
(6) Application of the flexural isostatic response to the remaining sedimentary section and basement.
(7) Sequential repetition of the above processes until all post-rift stratigraphic units have been removed.

This process is illustrated schematically in Fig. 4a. The flexural backstripping and reverse modelling process should not be carried back in time into the syn-rift stage or through periods of substantial erosion, as these processes violate the assumption of a closed entropy system required for reverse modelling. The restored post-rift (post-breakup) sections produced by flexural backstripping and reverse post-rift modelling, and their predicted palaeo-bathymetry or emergence are dependent on the β stretching factor (McKenzie, 1978) used to define the magnitude of lithosphere extension at rifting, and the flexural strength of the lithosphere. Lithosphere flexural strength may be parameterised by effective elastic thickness T_e. Flexural backstripping and reverse post-rift modelling may be used to predict palaeo-bathymetry from a knowledge of the β stretching factor, or to determine a β stretching factor from a knowledge of palaeo-bathymetry (Kusznir *et al*., 1994; Roberts *et al*., 1998).

Forward syn-rift modelling

The flexural cantilever model (Kusznir *et al*., 1991) has been used to forward model the syn-rift component of lithosphere deformation of the Lofoten margin occurring in the Late Cretaceous and Palaeocene prior to continental breakup and the development of sea-floor spreading. The flexural cantilever model describes the geometric, thermal and flexural isostatic response of the lithosphere to extension on planar faults in the upper crust and plastic distributed deformation in the lower crust and mantle (Fig. 4b).

During faulting, upper-crustal footwall and hangingwall blocks behave as two mutually self-supporting flexural cantilevers; their response to isostatic forces induced by extension generates footwall uplift and hanging wall collapse. For extension on multiple faults, the interference of footwall uplift and hangingwall collapse gives rise to the familiar half grabens, rotated fault blocks and horsts of rift tectonics that depend on fault polarity (Fig. 4c). The flexural cantilever model is able to predict crustal structure and sedimentary basin geometry for faults of arbitrary horizontal spacing, displacement and polarity. Within the flexural cantilever model, the plastic deformation in the lower crust and mantle are quantified by a 2D β stretching factor (McKenzie, 1978). Syn-rift thermal perturbation of the lithosphere temperature field and its post-rift thermal re-equilibration are computed from the 2D β stretching factor distribution. The model assumes that all loads

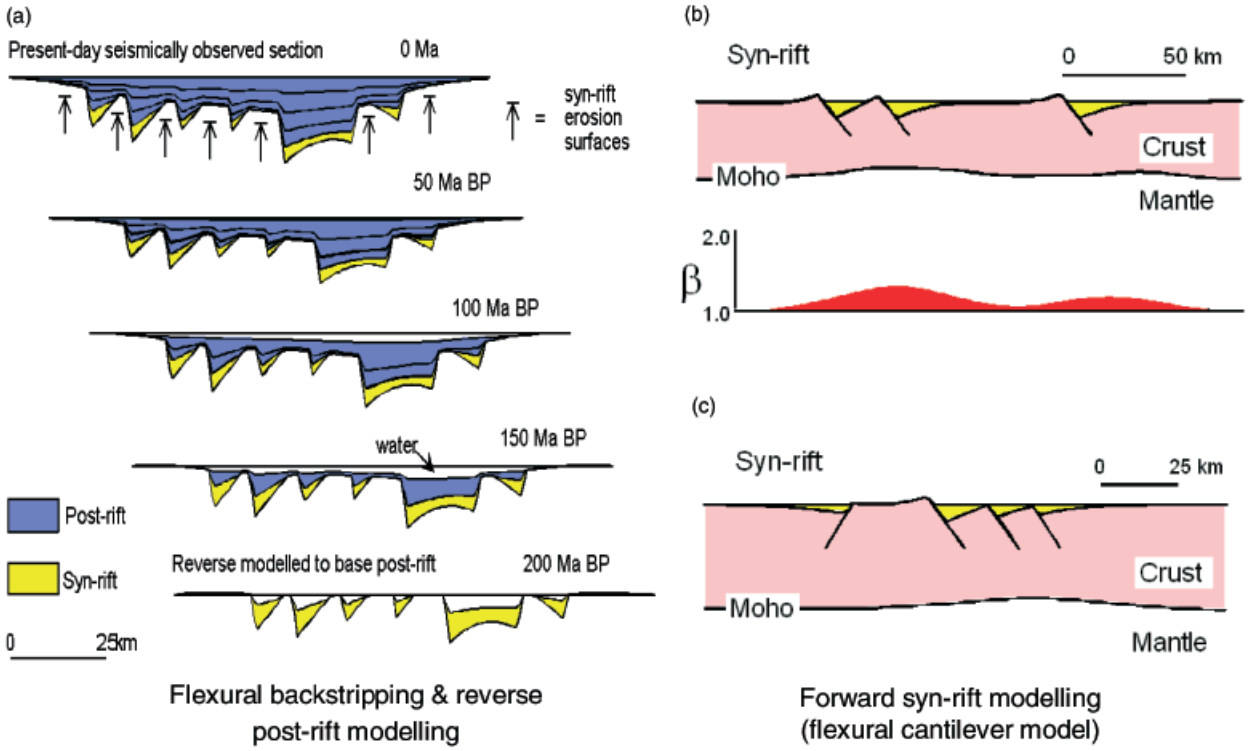

Fig. 4. (a) Schematic diagram showing application of flexural backstripping and reverse post-rift modelling to predict sequential restorations of post-rift stratigraphy and palaeo-bathymetry. Restored sections are dependent on the β stretching factor used to define the magnitude of lithosphere extension at rifting and lithosphere flexural strength. Flexural backstripping and reverse post-rift modelling may be used to determine β stretching factor from a knowledge of palaeo-bathymetry. (b) Schematic diagrams showing application of the flexural cantilever model of continental lithosphere extension to the syn-rift stage of basin development. Crustal extension of the upper crust on planar faults generates footwall uplift and hanging wall collapse. Plastic deformation in the lower crust and mantle are quantified by a 2D β stretching factor. (c) The interference of footwall uplift and hanging wall collapse gives rise to the familiar half-grabens, rotated fault blocks and horsts of rift tectonics depending on fault polarity.

generated by lithosphere extension associated with crustal thinning, syn-rift and post-rift thermal effects, sediment fill and erosional denudation are distributed using flexural isostasy. While the flexural cantilever model may be applied to forward modelling of post-rift basin development as well as syn-rift processes (see Kusznir & Ziegler, 1992; Nadin & Kusznir, 1995), reverse modelling of post-rift basin development is preferred since this allows observed sedimentary history to be used.

REVERSE POST-RIFT MODELLING OF POST-BREAKUP SUBSIDENCE FOR LINE 2: SOUTHERN LOFOTEN MARGIN

Flexural backstripping and reverse post-rift modelling has been used to produce a series of restored cross-sections for line 2 from present day to continental breakup at ~54 Ma corresponding to end Palaeocene–Early Eocene time.

Late Palaeocene transient regional uplift of amplitude 300 m is included in the model; this uplift is associated with the initiation of the main phase of igneous activity responsible for the North Atlantic Igneous Province (Nadin *et al.*, 1997; Roberts *et al.*, 1997). The reverse thermal subsidence model also includes residual thermal subsidence from an earlier Late Jurassic to Early Cretaceous rift with $\beta = 1.3$ and age 142 Ma. A value of $T_e = 3$ km has been used to define the flexural strength of the lithosphere for flexural backstripping and reverse post-rift modelling.

The preferred sequence of restorations at top Tare (54 Ma) is shown in Fig. 5 and uses a laterally varying lithospheric β factor that increases from 1 (no stretching) in the east to infinity on the western oceanic end of the profile. Reverse post-rift modelling with these parameters restores the top Tare to sea level at ~54 Ma in the west of the section consistent with palaeo-environmental evidence, while avoiding sub-aerial conditions and erosion at these times in the east of the section. The left central part of the section east of the basalts is predicted to be shallow marine at 54 and 54.1 Ma. Changing the timing of breakup from 54 to 65 Ma produces a restoration that fails to restore the top Tare to sea level at 54 Ma (Fig. 6).

Sensitivity to the lithosphere β factor used to define the reverse post-rift thermal subsidence model is shown in Fig. 7. Using a uniform β factor of 1 gives a satisfactory restoration at 54 Ma to the east of the Utrøst Ridge but predicts a large palaeo-bathymetry of ~2000 m in the west of the section in conflict with evidence of an emergent to shallow marine top Tare depositional environment.

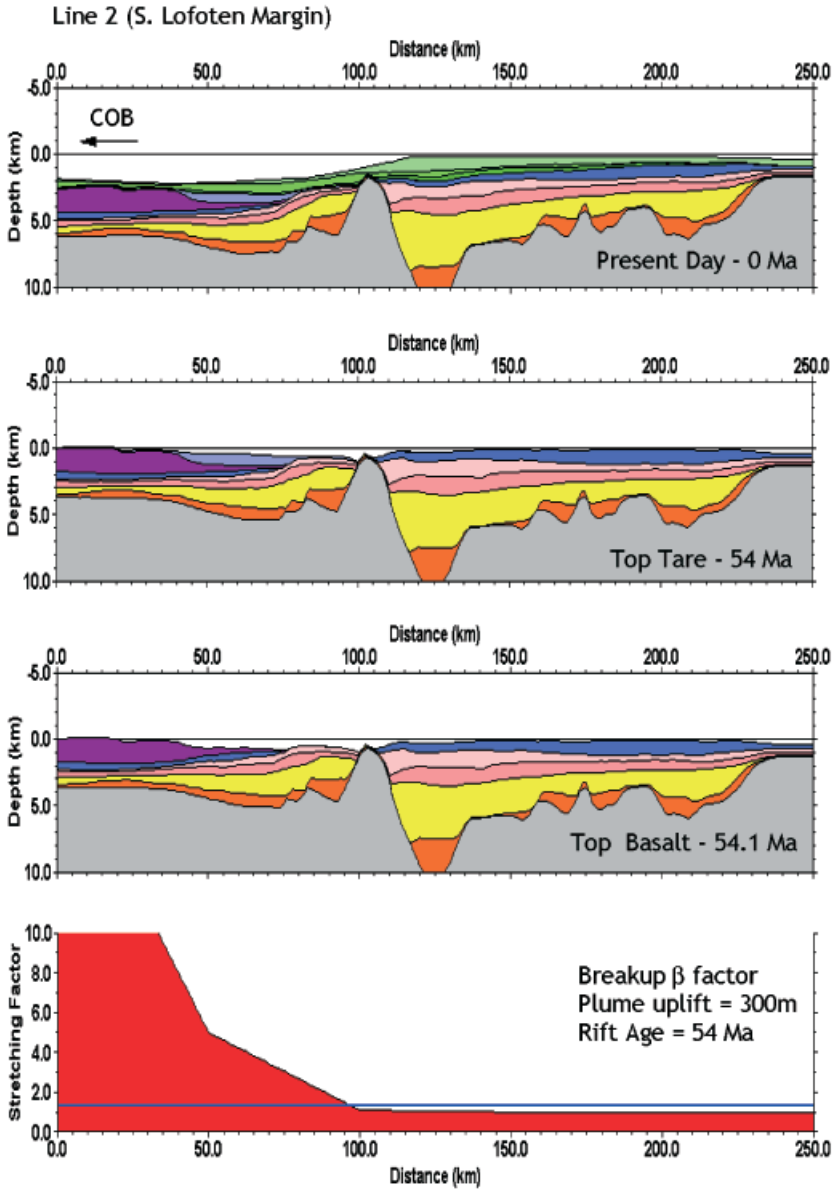

Fig. 5. Restored cross-sections for line 2 on the southern Lofoten margin produced by 2D flexural backstripping and reverse post-rift modelling from present day to top Tare at 54 Ma and top Basalt at 54.1 Ma. Rift age = 54.1 Ma. β stretching factor varies laterally decreasing from β = infinity for oceanic lithosphere to 1 in east. Transient mantle plume uplift for Upper Palaeocene = 300 m. Earlier Jurassic–Cretaceous rift at 142 Ma with β = 1.3. T_e = 3 km. The top Tare horizon is restored to sea level at ~54 Ma consistent with it fluvial depositional environment in the west.

Increasing the lithospheric β factor above 1 decreases the misfit of restored and observed bathymetry at top Tare time (~54 Ma) in the west of the section but elevates the restored section above sea level to the east of the Utrøst Ridge which would have led to erosion of Palaeocene and Cretaceous in this region, a feature not observed on this line. The preferred lithospheric β factor (Fig. 5) requires large values to the west of the Utrøst Ridge rapidly attenuating to 1 east of the Utrøst Ridge. The effect of increasing the transient uplift related to Upper Palaeocene igneous activity to 500 m produces a restoration that elevates the top Tare above sea level in the east of the section, a result that again is inconsistent with seismic observations from the line.

A sensitivity test of the effective elastic thickness, T_e, used to define the flexural strength of the lithosphere for reverse post-rift modelling is shown in Fig. 8. Restored cross-sections are shown for T_e = 0, 3, 10 and 25 km; T_e = 0 km corresponds to local isostasy. Because of the relatively long wavelength of the sediment and thermal loads, the restored cross-sections at top Tare are relatively insensitive to the value of T_e and predicted bathymetries for T_e = 0, 10 and 25 km differ very little from those for the preferred value of T_e = 3 km.

Although large β factors approaching infinity are required in the western part of the profile to generate a successful restoration there is no evidence for significant upper-crustal extension of Palaeocene or Eocene age.

PALAEOCENE EXTENSION AND SUBSIDENCE FOR LINE 2: SOUTHERN LOFOTEN MARGIN

Palaeo-environmental evidence suggests that palaeo-bathymetry was at or near sea level at the time of top Tare.

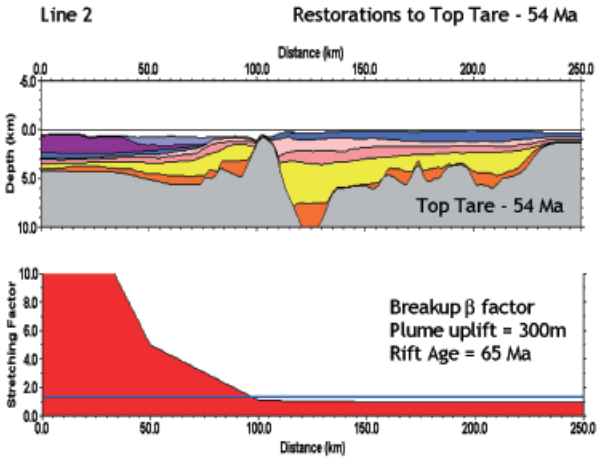

Fig. 6. Restored cross-section for line 2 on the southern Lofoten margin produced by 2D flexural backstripping and reverse post-rift modelling from present day to top Tare at 54 Ma using rift age = 65 Ma and the preferred lithosphere β stretching factor profile with β = infinity for the west of the profile. Transient mantle plume uplift for Upper Palaeocene = 300 m. Earlier Jurassic–Cretaceous rift at 142 Ma with β = 1.3. T_e = 3 km. A 65 Ma rift age fails to restore the top Tare to sea level as suggested by it depositional environment.

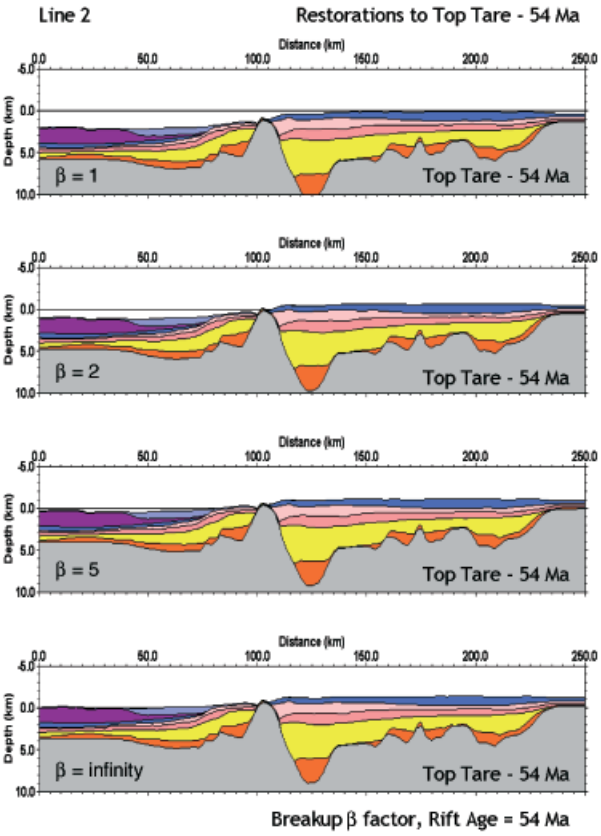

Fig. 7. Sensitivity tests of restored cross-sections to lithosphere β stretching factors for line 2 on the southern Lofoten margin. Restored cross-sections are shown for constant β factors of 1, 2, 5 and infinity and correspond to top Tare time (54 Ma). A β factor of infinity is required in the west of the profile to restore top Tare to sea level at 54 Ma. β factors of 1 are required in the east of the section in order to avoid elevating the eastern part of the section above sea level. All other modelling parameters are identical to those of the model shown in Fig. 5.

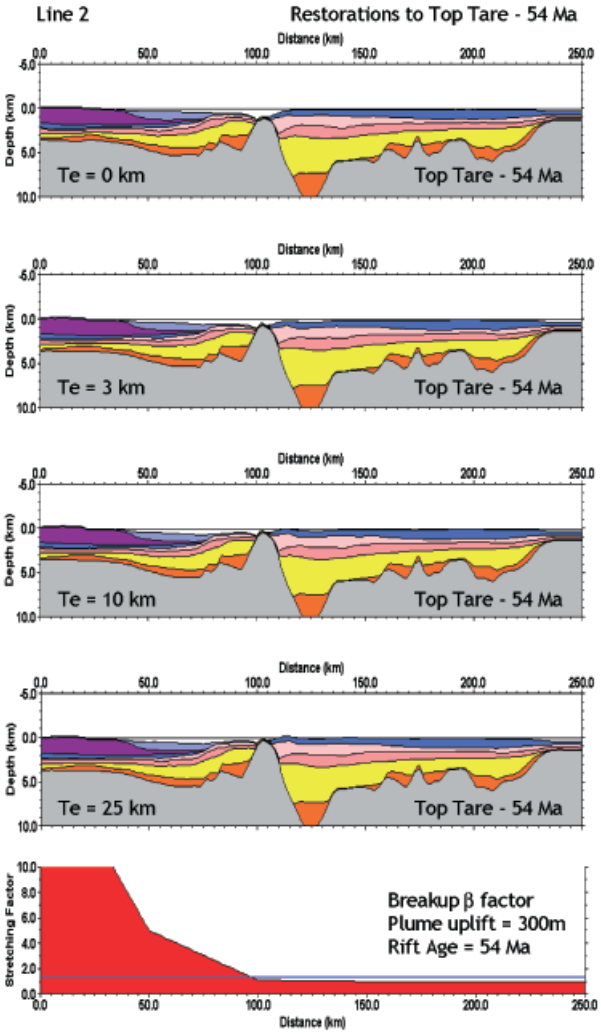

Fig. 8. Sensitivity tests of restored cross-sections to the effective elastic thickness, T_e, used to define the flexural strength of the lithosphere for line 2. Restored cross-sections are shown for T_e = 0, 3, 10 and 25 km, and correspond to top Tare time (54 Ma). Sections are reverse modelled using the preferred laterally varying β factor profile and other parameters identical to those of the model shown in Fig. 5. The restorations have very little sensitivity to T_e because of the relatively long wavelength of loads.

A sequence of restorations from 54 to 65 Ma has been produced starting with a section backstripped to top Tare time and flattened to sea level. The preferred restorations, shown in Fig. 9, use β = 1 for Palaeocene rifting (no rifting) and β = 1.3 at 142 Ma for the earlier Late Jurassic to Early Cretaceous rift. The restorations to 54.1, 58 and 65 Ma show a relatively flat surface at or near sea level. There is no sign of significant Palaeocene rifting. Some minor faulting can be seen at horizontal distances 20, 55 and 75 km. The restored surface at 58 and 65 Ma appears to be higher in the west than the east, with sub-aerial conditions in the west and shallow marine conditions in the east, consistent with well data further south (Dalland *et al.*, 1988; Eldholm *et al.*, 1989). Use of a β factor >1.05 in the restoration produces a restored upper surface above

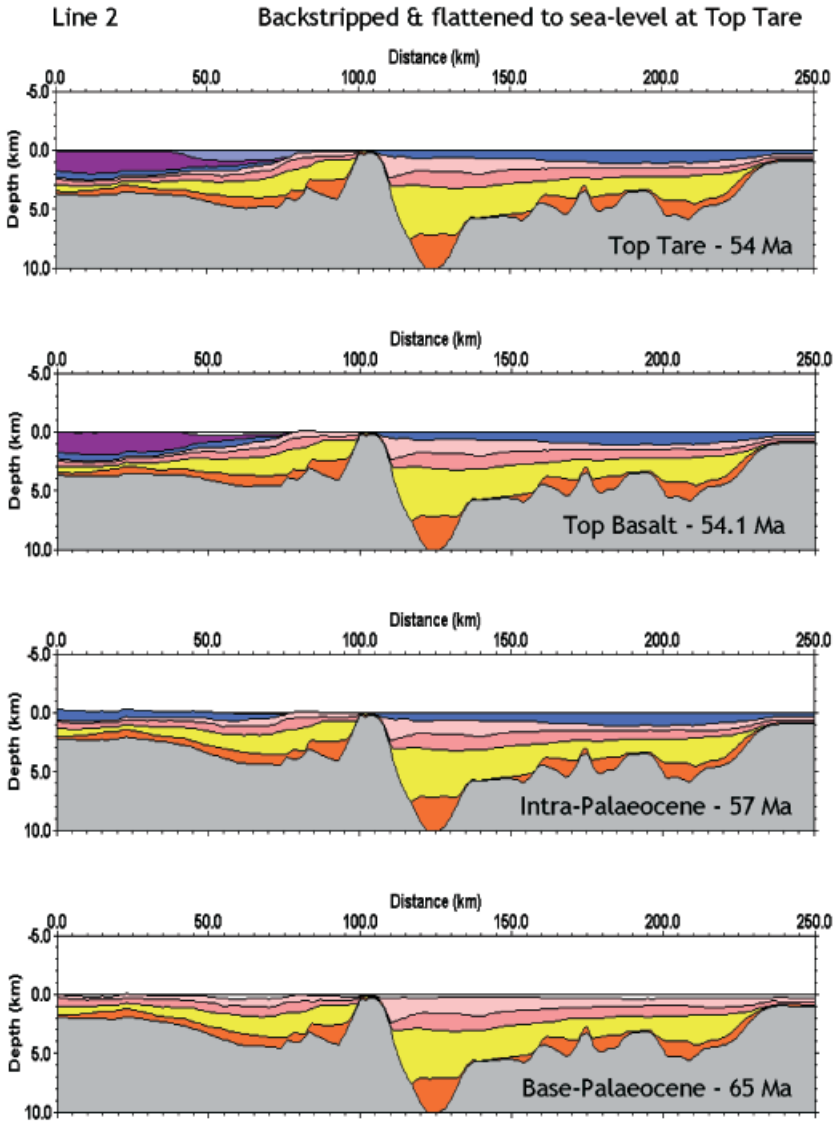

Fig. 9. Restored cross-sections for Lofoten line 2 from 54 to 65 Ma produced by flexural backstripping and reverse post-rift modelling from flattened section at 54 Ma. $\beta = 1$ (no stretching) for Early–Mid Palaeocene rift. Earlier Jurassic–Cretaceous rift at 142 Ma with $\beta = 1.3$. Transient mantle plume uplift for Upper Palaeocene = 300 m. $T_e = 3$ km. The restored sections show no significant faulting in the interval 54–65 Ma.

sea level that in the east, in particular, would be expected to generate substantial erosion of the Upper Cretaceous section. A similar restoration procedure to that above but starting with sea-level flattening at 58 Ma (Base Tare) and backstripping to 65 Ma also gives palaeo-bathymetries near sea level and no sign of significant Early Palaeocene rifting.

From the evidence above, the Early and Middle Palaeocene appears to have been a time of low lithospheric and upper-crustal extension.

LATE CRETACEOUS EXTENSION AND SUBSIDENCE FOR LINE 2: SOUTHERN LOFOTEN MARGIN

Reverse Post-rift modelling from 65 to 81.5 Ma

The results of flexural backstripping and reverse post-rift modelling from 65 to 81.5 Ma with a β factor of 1.05 for a Late Cretaceous rift at 81.5 Ma and $\beta = 1.3$ for an earlier rift at 142 Ma are shown in Fig. 10a. The starting point of the restoration is a backstripped section flattened to 200 m water depth at 65 Ma consistent with a marine depositional environment at this time. The restoration predicts Upper Cretaceous sediments below sea level in the interval 65–81.5 Ma, consistent with their marine depositional environment. Using a β greater than 1.05 for Late Cretaceous rifting produces invalid restorations in which the Late Cretaceous is elevated above sea level, which is inconsistent with its depositional environment as shown in wells further south in the northern Vøring Basin (Ren *et al.*, 2003). The upper bound of $\beta = 1.05$ is therefore suggested for Upper Cretaceous extension. The incremental development of accommodation space between the 65 and 81.5 Ma restorations shown in Fig. 10a indicates Late Cretaceous faulting in this time interval to the west of the Utrøst Ridge between horizontal distances 40 and 65 km, and on the large fault bounding the east side of the Utrøst Ridge.

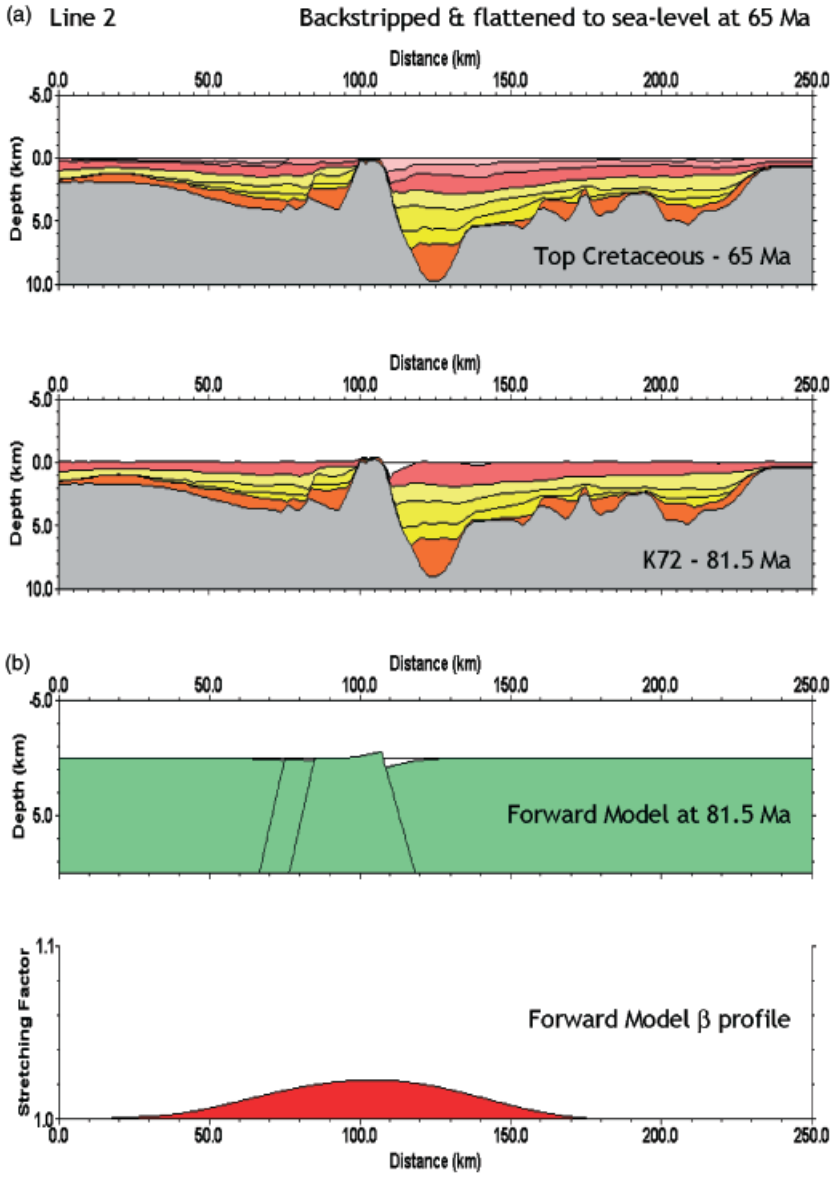

Fig. 10. (a) Restored cross-sections for Lofoten line 2 from 65 to 81.5 Ma produced by flexural backstripping and reverse post-rift modelling from flattened section at 65 Ma. $\beta = 1.05$ for Late Cretaceous rift with rift age = 81.5 Ma. Earlier Jurassic–Cretaceous rift at 142 Ma with $\beta = 1.3$. $T_e = 3$ km. The restored cross-section at 81.5 Ma shows evidence of minor faulting in the interval 65–81.5 Ma. (b) 2D syn-rift forward model of Late Cretaceous rifting for Lofoten line 2. Target stratigraphy derived by reverse post-rift modelling to 81.5 Ma (a). $T_e = 3$ km. The forward model predicts a maximum β factor of $\sim$1.03.

Forward syn-rift modelling of an Upper Cretaceous rift at 81.5 Ma

The results of using the flexural cantilever model to forward model Late Cretaceous extension as a single rift event at 81.5 Ma are shown in Fig. 10b. The target stratigraphy for the forward model is that derived from backstripping and flattening observed stratigraphy to 65 Ma and then reverse post-rift modelling to 81.5 Ma with a constant β factor of 1.05 at 81.5 Ma and an earlier rift at 142 Ma with $\beta = 1.3$. The forward model (Fig. 10b) of the Late Cretaceous rift gives a reasonable fit to the target stratigraphy and predicts a maximum β factor of $\sim$1.03. The forward model of Late Cretaceous rifting has fault movement only in the western part of the section. The most easterly fault moving at this time is the large fault bounding the east side of the Utrøst Ridge.

The results of reverse and forward modelling are consistent and predict that extensional faulting occurring in the Late Cretaceous interval 81–65 Ma had a maximum β stretching factor of no more than 1.05.

REVERSE POST-RIFT MODELLING OF POST-BREAKUP SUBSIDENCE FOR LINE 3: SOUTHERN LOFOTEN MARGIN

Line 3, the most northerly cross-section studied, lies on the southern Lofoten margin to the north of the Bivrøst lineament and fracture zone. Restored cross-sections for line 3 from present day to continental breakup at $\sim$54 Ma (top Tare) are shown in Fig. 11 for constant breakup lithosphere stretching factors of $\beta = 1$, 2, 5 and infinity. The restoration models include an earlier Late Jurassic to Early Cretaceous rift with $\beta = 1.3$ at 142 Ma, and a transient Early Palaeocene regional uplift of amplitude 300 m, similar

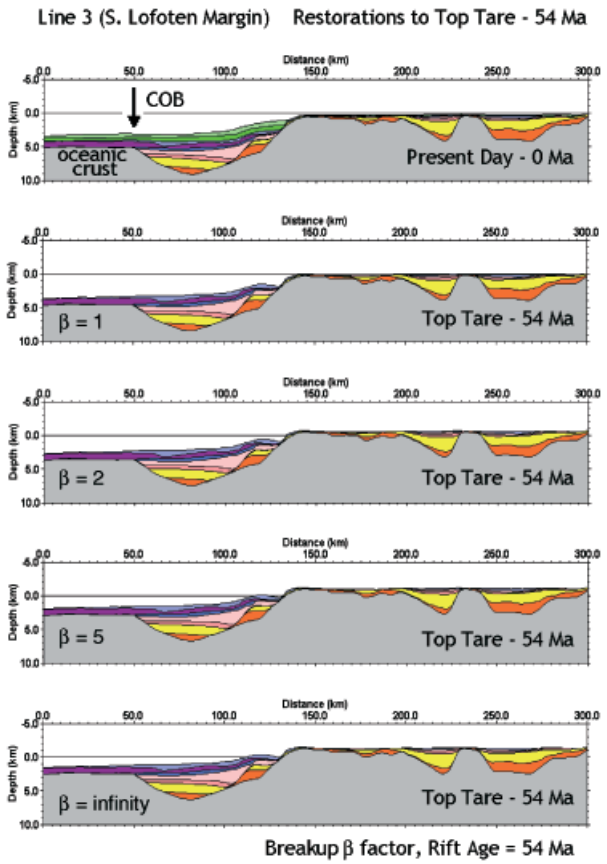

Fig. 11. Restored cross-sections produced by 2D flexural backstripping and reverse post-rift modelling from present day to top Tare at 54 Ma for line 3 on the southern Lofoten margin using constant β factors of 1, 2, 5 and infinity. In the west a β factor of infinity fails to restore top Tare to sea level at 54 Ma. In the east, a β factor of 1 is required of the section in order to avoid elevating the eastern part of the section above level. Transient mantle plume uplift for Upper Palaeocene = 300 m. Earlier Jurassic–Cretaceous rift at 142 Ma with β = 1.3. T_e = 3 km.

to that used for line 2. The COB is located at a horizontal distance of 50 km from the western end of the section.

Unlike the restoration for line 2, the use of a breakup lithosphere β stretching factor of infinity does not restore the top Tare horizon to sea level at ~54 Ma. The restoration with constant β = infinity predicts palaeo-bathymetries of ~1500 m in the western oceanic and oceanward 100 km of the section. For the eastern part of the section (to the east of the Utrøst Ridge) increasing β stretching factors above β = 1 gives predicted surface elevations increasingly above sea level, inconsistent with the deposition and preservation of Palaeocene and Late Cretaceous stratigraphy in this region.

A restoration using a laterally varying β factor for breakup at 54 Ma, which increases from β = 1 (no stretching) in the east to infinity on the western oceanic end of the profile is shown in Fig. 12a. This restoration again fails to elevate top Tare and top Basalt to sea level at ~54 Ma. The inclusion in the reverse model of 1500 m of (water loaded) Late Palaeocene transient mantle plume uplift (Fig. 12b) does restore the top Tare and top Basalt to sea-level horizon at ~54 Ma. However, this amplitude of transient plume uplift is thought to be unreasonably large with respect to that required to produce adequate restoration elsewhere in the North Atlantic (Nadin & Kusznir, 1995; Nadin *et al.*, 1997; Roberts *et al.*, 1997). Furthermore, incorporating this amount of uplift elevates the central and eastern parts of the cross-section to ~1000–1500 m above sea level, which would have resulted in erosion and removal of Palaeocene and Late Cretaceous sequences. Although erosion of the Palaeogene section is seen in this area (Fig. 3) a restoration involving 1500 m of transient uplift associated with Late Palaeocene magmatism is considered unlikely. The magnitude and cause of uplift and erosion in this part of the Lofoten margin remains unresolved.

If the evidence for zero bathymetry or emergence of the top Tare and top Basalt horizons at ~54 Ma based on ODP and DSDP well observations seen to the SW can be extrapolated to line 3, then a satisfactory restoration of the top Tare and top Basalt to sea level at ~54 Ma requires the inclusion of an additional subsidence event younger than top Tare (54 Ma). If the top Tare and top Basalt horizons were deposited at sea level at ~54 Ma, the long wavelength of the bathymetric anomaly west of the Utrøst Ridge precludes an origin involving upper-crustal faulting to the west of the Utrøst Ridge. A possible mechanism for additional post 54 Ma long-wavelength subsidence is thinning of the lower continental crust west of the Utrøst Ridge during the Early Eocene. Thinning of the lower crust during sea-floor spreading initiation or early sea-floor spreading would have resulted in additional subsidence to that from generated by post-breakup thermal subsidence. The large extensional fault at distance 135 km from the western end of the section (and bounding the western side of the northern end of the Utrøst Ridge) may have also moved at this time. There is no evidence of any other significant upper-crustal faulting and extension in the Eocene (or Palaeocene). An alternative mechanism for generating the additional post-breakup subsidence on Lofoten line 3 is the evacuation of lower-crustal melt during early sea-floor spreading. While lower-crustal magmatic underplating bodies (LCBs) exist on the Vøring segment of the Norwegian Margin south of the Bivrøst Lineament, similar lower-crustal magmatic bodies appear to be much less well developed on the Lofoten margin segment (Mjelde *et al.*, 1993; Tsikalas *et al.*, 2001).

Alternatively, it may be that the evidence for zero palaeo-bathymetry at top Tare and top Basalt times seen in ODP and DSDP wells to the SW may not be extrapolated to line 3, and that top Tare and top Basalt depositional palaeo-bathymetries were of the order of ~1500 m. Planke *et al.* (2000) and Berndt *et al.* (2001) have presented evidence based on volcanic seismic facies data on the northern Vøring and southern Lofoten margins for extrusive volcanism occurring not only sub-aerially (or at sea level) but also in a shallow marine environment. It is worth noting that the palaeo-bathymetries of ~1500 m predicted for top Tare and top Basalt at ~54 Ma (Fig. 12) for oceanic

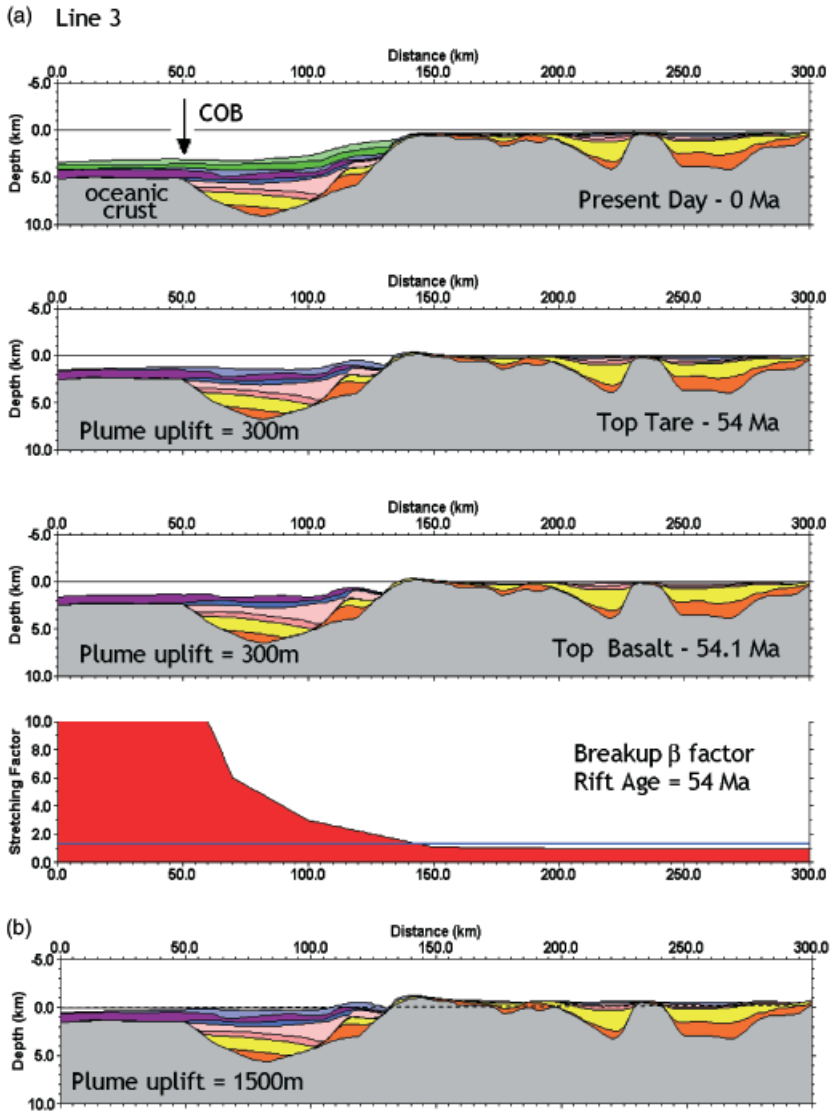

Fig. 12. (a) Restored cross-sections for line 3 on the southern Lofoten margin produced by 2D flexural backstripping and reverse post-rift modelling from present day to top Tare at 54 Ma and top Basalt at 54.1 Ma. Rift age = 54.1 Ma. β stretching factor varies laterally decreasing eastwards from β = infinity for oceanic lithosphere to 1 in east. Other modelling parameters are identical to those of the model shown in Fig. 10. Restored palaeo-bathymetry of 1500 m is predicted to the west of $x = 130$ km at 54 Ma; the top Tare does not restore to sea level at ~54 Ma and may imply an additional subsidence event younger than 54 Ma. (b) Restored cross-sections for line 3 produced by 2D flexural backstripping and reverse post-rift modelling from present day to top Tare and top Basalt at 54.1 Ma using a transient mantle plume uplift for Upper Palaeocene = 1500 m. The larger transient plume uplift of 1500 m predicts zero top Tare palaeo-bathymetry at 54 Ma but elevates the eastern part of the section ($x > 140$ km) too high above sea level. β stretching factor and other parameters are identical to those of (a).

crust on the westernmost 50 km of the restored line 3 cross-section are consistent with palaeo-bathymetries expected for young oceanic crust with greater than average crustal thicknesses generated by sea-floor spreading in the vicinity of a mantle plume (White & McKenzie, 1989, 1995).

POST-BREAKUP, PALAEOCENE AND LATE CRETACEOUS EXTENSION AND SUBSIDENCE FOR LINE 1: NORTHERN VØRING MARGIN

Line 1 is located on the northern Vøring margin to the south of the Bivrøst lineament. The restoration to top Tare time for line 1 produced by reverse post-breakup modelling from the present day section is illustrated in Fig. 13 together with the preferred breakup lithosphere β stretching factor profile. The restoration successfully restores top Tare to sea level at 54 Ma and requires a lithosphere β stretching factor decreasing from ~2.5 near the continent-ocean boundary to 1 in the east of the section. The magnitude of lithosphere β stretching factor (~2.5) in the western part of line 1 is much less than the magnitudes for lines 2 and 3 in the equivalent location with respect to the continent ocean boundary, suggesting a marked change in the form of lithosphere stretching across the Bivrøst Lineament.

Reverse and forward stratigraphic modelling of Palaeocene and Late Cretaceous rifting for line 1 is illustrated in Fig. 14 and shows that combined Palaeocene and Late Cretaceous extension has a maximum stretching factor of β = 1.1 which is greater than that for lines 2 and 3. The magnitude of Palaeocene upper-crustal extension preceding breakup is however extremely small. These results are consistent with those of Roberts *et al.* (1997) for the Vøring margin.

DISCUSSION AND SUMMARY

The southern Lofoten and northern Vøring rifted margin shows extremely large stretching factors for continental

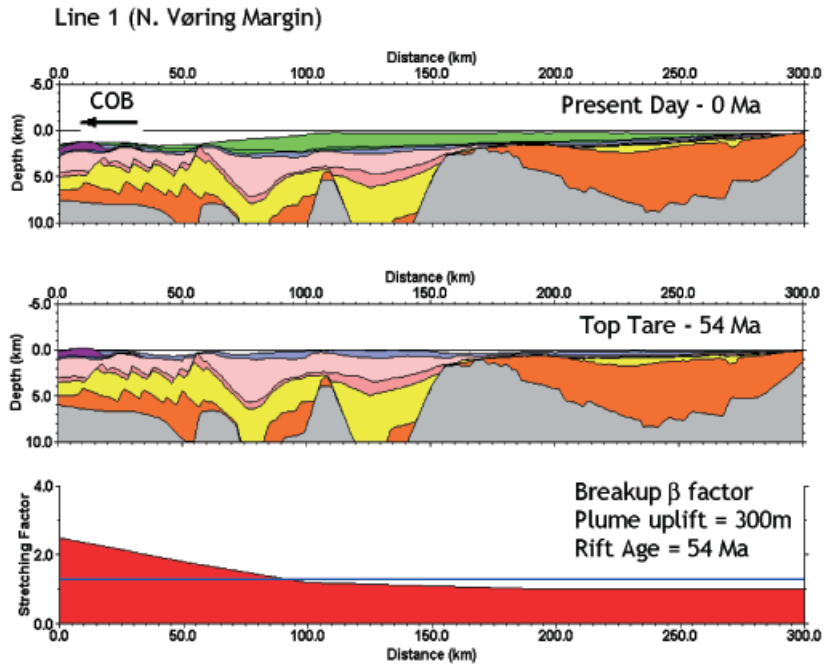

Fig. 13. Restored cross-sections for line 1 on the northern Vøring margin produced by 2D flexural backstripping and reverse post-rift modelling from present day to top Tare at 54 Ma. Rift age = 54.1 Ma. β stretching factor varies laterally decreasing eastwards from β = 2.5 in the west to 1 in east. The top Tare horizon is restored to sea level at ∼ 54 Ma consistent with sub-aerial depositional environment in the west. Transient mantle plume uplift for Late Palaeocene = 300 m. Earlier Jurassic–Cretaceous rift at 142 Ma with β = 1.3. T_e = 3 km.

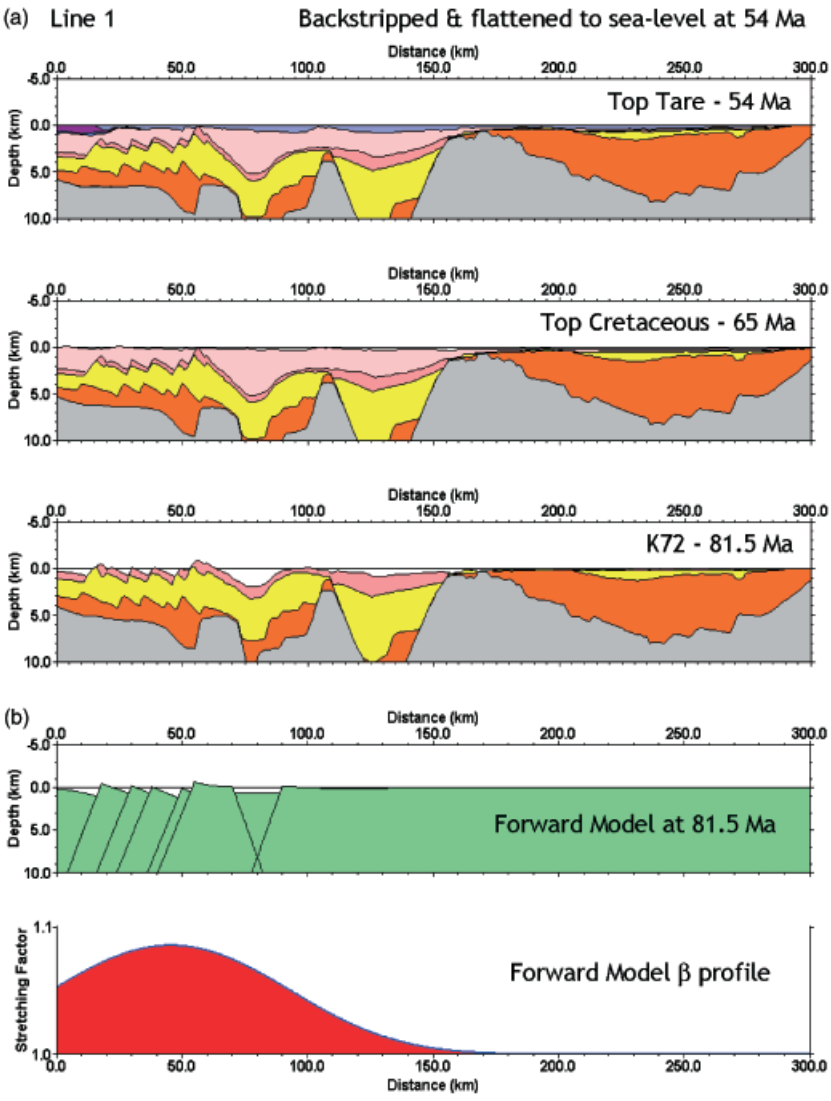

Fig. 14. (a) Restored cross-sections for line 1 on the northern Vøring margin from 54 to 81.5 Ma produced by flexural backstripping and reverse post-rift modelling from flattened section at 54 Ma. β = 1.1 for Late Cretaceous rift with rift age = 81.5 Ma. Earlier Jurassic–Cretaceous rift at 142 Ma with β = 1.3. T_e = 3 km. The restored cross-section at 81.5 Ma shows evidence of minor faulting in the interval 54–81.5 Ma. (b) 2D syn-rift forward model of Late Cretaceous rifting for line 1. Target stratigraphy derived by reverse post-rift modelling to 81.5 Ma (Fig. 14a). T_e = 3 km. The forward model predicts a maximum β factor of ∼1.1.

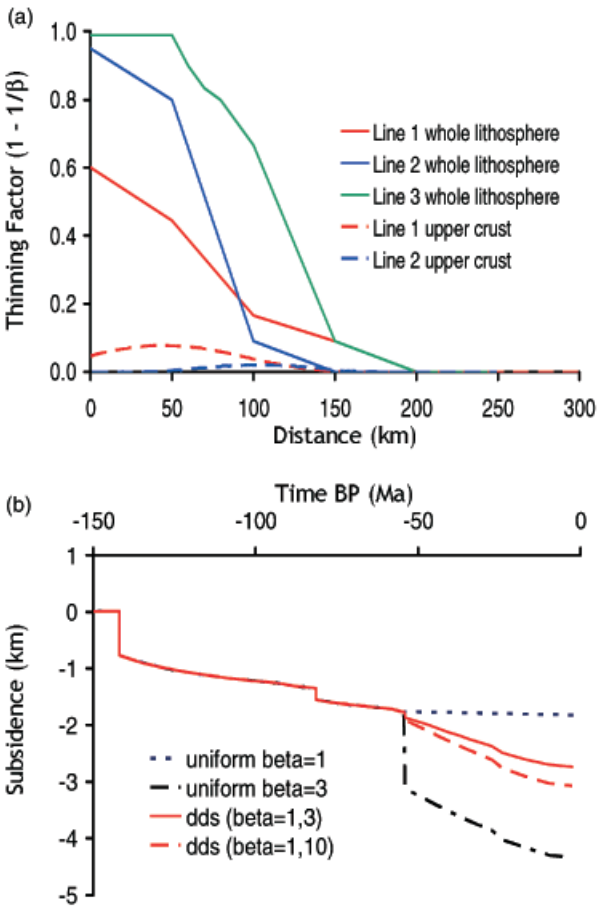

Fig. 15. (a) Summary and comparison of thinning factor $(1 - 1/\beta)$ profiles for whole-lithosphere and upper-crustal stretching for lines 1, 2 and 3 showing depth-dependent lithosphere stretching on the southern Lofoten and northern Vøring continental margins. Pre-breakup upper-crustal stretching in Late Cretaceous and Palaeocene ($\beta < 1.1$) is much less than lithosphere stretching at breakup ($\beta = 2.5$ to infinity). Lithosphere stretching and thinning on the southern Lofoten continental margin is greater than that on the northern Vøring margin. (b) Sensitivity of rifted margin water-loaded subsidence history to lithosphere depth-dependent stretching predicted by 1D model. Breakup age = 54 Ma. Earlier depth uniform lithosphere stretching at 142 and 81 Ma with $\beta = 1.3$ and 1.1 respectively. Depth-dependent stretching at 54 Ma with $\beta = 1$ for upper crust and $\beta = 3$ and also $\beta = 10$ for lower crust and mantle generates little syn-breakup subsidence compared with depth uniform stretching with = 3 and 10.

margin lithosphere at breakup at ~54 Ma with β approaching infinity towards the COB for the southern Lofoten margin and $\beta \sim 2.5$ for the northern Vøring margin. In contrast, upper-crustal extension for both the southern Lofoten and northern Vøring rifted margins at breakup at ~54 Ma and in the Palaeocene preceding breakup is very small, and substantially less than the combined Palaeocene and Late Cretaceous β stretching factors for the southern Lofoten and northern Vøring rifted margins of 1.05 and 1.1, respectively. Profiles of thinning factor $(1 - 1/\beta)$ for whole-lithosphere stretching and thinning, and that of the upper crust, are summarised for lines 1, 2 and 3 in Fig. 15a. Both the southern Lofoten and northern Vøring rifted margins show depth-dependent lithosphere stretching at breakup in which whole-lithosphere stretching and thinning greatly exceeds that of the upper crust. Wide-angle seismic and gravity studies show that the continental crust at the outer part of the margin is greatly thinned (Mjelde *et al.*, 1993, 1998; Skogseid *et al.*, 2000; Tsikalas *et al.*, 2001). The absence of upper-crustal fault extension and large magnitude whole-lithosphere thinning at breakup is consistent with depth-dependent stretching occurring during sea-floor spreading initiation and early sea-floor spreading. The Norwegian Margin appears to be segmented across the Bivrøst Lineament. Whole-lithosphere stretching north of the Bivrøst Lineament on the Lofoten Margin segment is greater than that to the south on the Vøring segment. However, on the Lofoten segment the lithosphere stretching attenuates very abruptly east of the Utrøst Ridge.

The implications of depth-dependent lithosphere stretching on post-breakup rifted margin subsidence history are shown in Fig. 15b. Water-loaded subsidence is computed for a 1D continental lithosphere model incorporating crustal thinning, lithosphere geotherm perturbation and re-equilibration, and their isostatic consequences in response to depth-dependent stretching. Predicted subsidence histories are compared for depth uniform lithosphere stretching at continental breakup at 54 Ma with $\beta = 1$ (no stretching) and $\beta = 3$, and for depth-dependent stretching with $\beta = 1$ for the upper crust and $\beta = 3$ and 10 for the lower crust and lithospheric mantle. The two depth-dependent models schematically represent the breakup stretching and thinning of the northern Vøring and southern Lofoten rifted margins. The 1D model has an initial crustal thickness of 35 km and includes earlier Late Jurassic–Early Cretaceous rifting at 142 Ma with $\beta = 1.3$, and Late Cretaceous rifting at 82 Ma with $\beta = 1.1$. The predicted subsidence for the depth-dependent stretching model with $\beta = 1$ for the upper crust and $\beta = 3$ for the lower crust and mantle at breakup shows little syn-breakup (i.e. syn-rift) subsidence at 54 Ma compared with the depth uniform model with $\beta = 3$. The post-breakup thermal subsidence is, however, only slightly less than that of the depth uniform stretching model. For the depth-dependent stretching model, subsidence from crustal thinning is reduced with respect to the depth uniform model. For the example of depth-dependent lithosphere stretching shown in Fig. 15b, the reduced crustal thinning subsidence at breakup approximately balances the thermal uplift due to increased lithosphere geothermal gradient with the result that there is little syn-breakup subsidence. This isostatic response to depth-dependent stretching may explain the relatively low palaeo-bathymetries observed during continental breakup on the Norwegian margin. The subsidence response to depth-dependent stretching with $\beta = 10$ for the lower crust and lithospheric mantle also shows little syn-breakup subsidence, but does show an increased

post-breakup thermal subsidence. The syn-breakup subsidence response to depth-dependent stretching is dependent on the crustal thickness at breakup; increasing crustal thickness increases syn-breakup subsidence while decreasing crustal thickness leads to syn-breakup uplift. Modelling shows that the syn-breakup subsidence on the Norwegian margin is therefore dependent on the magnitude of the earlier Late Jurassic–Early Cretaceous and Late Cretaceous rifting events.

Recent observations of depth-dependent stretching at both non-volcanic and volcanic margins, where upper-crustal extension is much less than that of the lower crust and lithospheric mantle (Roberts *et al*., 1997; Driscoll & Karner, 1998; Davis & Kusznir, 2004), and the discovery of broad domains of exhumed continental mantle at non-volcanic rifted margins (Pickup *et al*., 1996; Manatschal & Nievergelt, 1997; Minshull *et al*., 1998; Manatschal & Bernoulli, 1999; Whitmarsh *et al*., 2001) are not predicted by existing quantitative models of rifted margin formation based on intra-continental rift models subjected to very large stretching factors (e.g. Le Pichon & Sibuet, 1981). Simple fluid flow models of sea-floor spreading initiation within continental lithosphere using analytical iso-viscous corner-flow solutions (Kusznir & Tymms, 2003; Kusznir & Karner, in press) show that the divergent motion of the upwelling mantle beneath the developing sea-floor spreading centre generates depth-dependent stretching and thinning of the young continental margin. The observations on the Lofoten and Vøring rifted margins of depth-dependent lithosphere stretching and thinning, and the absence of significant Palaeocene or Late Cretaceous upper-crustal faulting are consistent with depth-dependent continental lithosphere stretching at rifted margins occurring during early sea-floor spreading initiation and early sea-floor spreading. The Lofoten and Vøring margin observations, together with the fluid-flow models of sea-floor spreading initiation, suggest that the dominant process responsible for the depth-dependent thinning of rifted continental margin lithosphere is sea-floor spreading initiation and early sea-floor spreading, rather than pre-breakup intra-continental rifting.

The possible identification on the southern Lofoten margin of additional continental margin subsidence due to lower-crustal thinning during early sea-floor spreading is also consistent with this hypothesis. If ODP and DSDP well evidence for zero bathymetry for top Tare and top Basalt deposition at $\sim$54 Ma can be extrapolated northwards to line 3, post-breakup thermal subsidence alone is not able to explain observed post-breakup subsidence of the rifted continental margin at the oceanic end of line the profile, and an additional subsidence event younger than 54 Ma is required. A possible mechanism to generate this additional subsidence, which has a long wavelength and is not generated by upper-crustal faulting, may be thinning of the lower continental crust during sea-floor spreading initiation and early sea-floor spreading.

ACKNOWLEDGEMENTS

We thank ConocoPhillips for allowing us to publish the work described in this paper, Ian Prince for providing stratigraphic data, and Filoppos Tsikalas and Elizabeth Eide for providing the maps shown in Fig. 1, and reviewers for their constructive comments. We also thank Christian Berndt, Mark Davis, Mike Cheadle, Neil Driscoll, Garry Karner, Eric Lundin, Tim Minshull and Bob Whitmarsh for helpful and stimulating discussions.

REFERENCES

Baxter, K., Cooper, G.T., Hill, K.C. & O'Brian, G.W. (1999) Late Jurassic subsidence and passive margin evolution in the Vulcan Sub-basin, north-west Australia: constraints from basin modelling. *Basin Res.*, **11**, 97–111.

Berggren, W.A., Kent, D.V., Swisher, C.C. III & Aubry, M.P. (1995) A revised Cenozoic geochronology and chronostratigraphy. In: *Geochronology, Time Scales and Global Stratigraphic Correlation* (Ed. by W.A. Berggren, D.V. Kent, CC. Swisher III & J Hardenol), *Soc. Sediment. Geol. (SEPM) Spec. Publ.*, **54**, 129–212.

Berndt, C., Planke, S., Alvestad, E., Tsikalas, & Rasmussen, T. (2001) Seismic volcanostratigraphy of the Norwegian margin: constraints on break-up process. *J. Geol. Soc. London*, **158**, 413–426.

Blystad, P., Brekke, H., Færseth, R.B., Larsen, B.T., Skogseid, J. & Tørudbekken, B. (1995) Structural elements of the Norwegian continental shelf. Part II: the Norwegian Sea Region. *NPD, Norw. Petrol. Directorate Bull.*, **8**, 45.

Brekke, H. (2000) The tectonic evolution of the Norwegian Sea continental margin with emphasis on the Vøring and Møre Basins. In: *Dynamics of the Norwegian Margin* (Ed. by A. Nøttvedt) *Geol. Soc. London Spec. Publ.*, **167**, 327–378.

Cande, S.C. & Kent, D.V. (1992) A new geomagnetic timescale for the Late Cretaceous and Cenozoic. *J. Geophys. Res.*, **97**, 13917–13951.

Caston, V.N.D. (1976) Tertiary sediments of the Vøring Plateau, Norwegian Sea, recovered by Leg 38 of the Deep Sea Drilling Project. In: *Initial Reports of the Deep Sea Drilling Project* (Ed. by M. Talwani & G. Udintsev, *et al.*) *US Government Printing Office Washington*, **38**, 1101–1168.

Dalland, A., Worsley, W. & Ofstad, K. (1988) A lithostratigraphic scheme for the Mesozoic and Cenozoic succession offshore mid- and northern Norway. *NPD, Norw. Petrol. Directorate Bull.*, **4**, 65.

Davis, M. & Kusznir, N.J. (2004) Depth-dependent lithospheric stretching at rifted continental margins. In: *Proceedings of NSF Rifted Margins Theoretical Institute* (Ed. by G.D Karner), pp. 92–136. Columbia University Press, New York.

Doré, A.G., Lundin, E.R., Jensen, L.N., Birkeland, O., Eliassen, P.E. & Fichler, C. (1999) Principal tectonic events in the evolution of the northwest European Atlantic margin. In: *Petroleum Geology of Northwest Europe: Proceedings of the 5th Conference* (Ed. by A.J. Fleet & S.A.R. Boldy), pp. 41–61. Geological Society, London.

Driscoll, N. & Karner, G. (1998) Lower crustal extension across the Northern Carnarvon basin, Australia: evidence for an eastward dipping detachment. *J. Geophys. Res.*, **103**, 4975–4991.

Eide, E.E. (2002) *BATLAS – Mid Norway Plate Reconstruction Atlas with Global and Atlantic Perspectives*. Geological Survey of Norway, Norway.

Eldholm, O., Skogseid, J., Planke, S. & Gladczenko, T.P. (1995) Volcanic margin concepts. In: *Rifted Ocean–Continent Boundaries* (Ed. by E. Banda), pp. 1–16. Kluwer, Dordrecht, Netherlands.

Eldholm, O., Thiede, J. & Taylor, E. (1989) Evolution of the Vøring Volcanic Margin. In: *Proceedings of the Ocean Drilling Program, Scientific Results* (Ed. by O. Eldholm, J. Thiede & E. Taylor, *et al.*), *Ocean Drilling Program, College Station, TX,* **104**, 1033–1065.

Gradstein, F.M., Agterberg, F.P., Ogg, J.G., Hardenbol, J., van Veen, P., Thierry, J. & Huang, Z. (1994) A Mesozoic time scale. *J. Geophys. Res.*, **99**, 24051–24074.

Kusznir, N.J. & Karner, G.D. Modelling sea-floor spreading initiation and rifted continental margin formation: Does depth dependent stretching occur pre- or syn-breakup? *EOS Trans. AGU*, in press.

Kusznir, N.J., Marsden, G. & Egan, S.S. (1991) A flexural cantilever simple-shear/pure-shear model of continental lithosphere extension: Application to the Jeanne D'Arc basin, Grand banks and Viking Graben North Sea. In: *Geometry of Normal Faults* (Ed. by A.M. Roberts, G. Yielding & B. Freeman), *Geol. Soc. London Spec. Publ.*, **56**, 41–60.

Kusznir, N.J., Roberts, A. & Morley, C. (1994) Forward and reverse modelling of rift basin formation. In: *Hydrocarbon Habitat in Rift Basins* (Ed. by J. Lambiase), *Geol. Soc. London Spec. Publ.*, **80**, 33–56.

Kusznir, N.J. & Tymms, V. (2003) Modelling sea floor spreading initiation and depth dependent stretching at rifted continental margins. *EOS Trans. AGU*, **84**, 1342.

Kusznir, N.J. & Ziegler, P.A. (1992) The mechanics of continental extension and sedimentary basin formation – a simple-shear pure-shear flexural cantilever model. *Tectonophysics*, **215**, 117–131.

Le Pichon, X. & Sibuet, J.C. (1981) Passive margins: a model of formation. *J. Geophys. Res.*, **86**, 3708–3720.

Lundin, E.R. & Doré, A.G. (1997) A tectonic model for the Norwegian passive margin with implications for the NE Atlantic Early Cretaceous to break-up. *J. Geol. Soc. London*, **154**, 545–550.

Manatschal, G. & Bernoulli, D. (1999) Architecture and tectonic evolution of nonvolcanic margins: present day Galicia and ancient Adria. *Tectonics*, **18**, 1099–1119.

Manatschal, G. & Nievergelt, P. (1997) A continent–ocean transition recorded in the Err and Platta nappes (Eastern Switzerland). *Eclogae Geol. Helv.*, **90**, 3–27.

McKenzie, D.P. (1978) Some remarks on the development of sedimentary basins. *Earth Planet. Sci. Lett.*, **40**, 25–32.

Minshull, T.A., Dean, S.M., White, R.S. & Whitmarsh, R.B. (1998) Restricted melting at the onset of seafloor spreading: ocean–continent transition zones at non-volcanic rifted margins. *EOS Trans. AGU*, **79**, 906.

Mjelde, R., Digranes, P., Shimamura, H., Shiobara, H., Kodira, S., Brekke, H., Egebjerg, T., Sørnes, N. & Thorbjørnsen, S. (1998) Crustal structure of the northern part of the Vøring Basin, mid-Norway margin, from wide-angle seismic and gravity data. *Tectonophysics*, **293**, 175–205.

Mjelde, R., Sellevoll, M.A., Shimamura, H., Iwasaki, T. & Kanazawa, T. (1993) Crustal stucture beneath Lofoten, N. Norway, from vertical incidence and wide-angle seismic data. *Geophys. J. Int.*, **114**, 116–126.

Mosar, J. & Torsvik, T.H.& the BAT team (2002) Opening the Norwegian and Greenland Seas: plate tectonics in Mid Norway since the Late Permian. In: *BATLAS - Mid Norway Plate Reconstruction Atlas with Global and Atlantic Perspectives* (Ed. by E.E. Eide), pp. 48–59. Geological Survey of Norway, Norway.

Nadin, P.A. & Kusznir, N.J. (1995) Palaeocene uplift and Eocene subsidence in the northern North Atlantic from 2D forward and reverse stratigraphic modelling. *J. Geol. Soc. London*, **152**, 833–848.

Nadin, P., Kusznir, N.J. & Cheadle M, J. (1997) Early Tertiary plume uplift in the North Sea and Faeroe-Shetland Basin. *Earth Planet. Sci. Lett.*, **148**, 109–127.

Pickup, S.L.B., Whitmarsh, R.B., Fowler, C.M.R. & Reston, T.J. (1996) Insight into the nature of the ocean–continent transition off West Iberia from a deep multichannel seismic reflection profile. *Geology*, **24**, 1079–1082.

Planke, S., Symonds, P., Alvestad, E. & Skogseid, J. (2000) Seismic volcano-stratigraphy of large-volume basalt extrusive complexes on rifted margins. *J. Geophys. Res.*, **105**, 19335–19351.

Price, S., Brodie, J., Whitham, A. & Kent, R. (1997) Mid-Tertiary rifting and magnetism in the Traill Ø region, East Greenland. *J. Geol. Soc. London*, **154**, 419–434.

Ren, S., Faleide, J.I., Eldholdm, O., Skogseid, J. & Gradstein, F. (2003) Late Cretaceous–Palaeocene tectonic development of the NW Vøring Basin. *Marine Petrol. Geol.*, **20**, 177–206.

Riis, F. & Fjeldskaar, W. (1992) On magnitude of the late Tertiary and Quaternary erosion and its significance for the uplift of Scandinavia and the Barents Sea. In: *Structural and Tectonic Modelling and its Application to Petroleum Geology* (Ed. by R.M. Larsen, H. Brekke, B.T. Larsen & E. Talleraas), *Spec. Publ. Norw. Petrol. Soc.*, **1**, 163–185.

Roberts, A.M., Kusznir, N.J., Yielding, G. & Styles, P. (1998) Backstripping extensional basins: the need for a sideways glance. *Petrol. Geosci.*, **4**, 327–338.

Roberts, A.M., Lundin, E.R. & Kusznir, N.J. (1997) Subsidence of the Vøring Basin and the influence of the Atlantic continental margin. *J. Geol. Soc. London*, **154**, 551–557.

Roberts, D.G., Thompson, M., Mitchener, B., Hossack, J., Carmichael, S.M.M. & Bjornseth, H.M. (1999) Palaeozoic to Tertiary rift and basin dynamics; mid-Norway to the Bay of Biscay; a new context for hydrocarbon prospectivity in the deep water frontier. In: *Petroleum Geology of Northwest Europe: Proceedings of the 5th Conference* (Ed. by A.J. Fleet & S.A.R. Boldy), pp. 7–40. Geological Society, London.

Saunders, A.D., Fitton, J.G., Kerr, A.C., Norry, M.J. & Kent, R.W. (1997) The North Atlantic igneous province. In: *Large Igneous Provinces* (Ed. by J.J. Mahoney & M.F. Coffin), *Geophys. Monograph, AGU*, **100**, 45–93.

Sigmond, E.M.O. (2002) Geological map, land and sea areas of Northern Europe. Scale 1:3 million. *Geol. Surv Norway.*

Sinton, C.W., Hitchen, K. & Duncan, R.A. (1998) 40Ar–39Ar geochronology of silicic and basic volcanic rocks. *Geol. Mag*, **135**, 161–170.

Skogseid, J., Planke, S., Faleide, J.I., Pedersen, T., Eldholm, O. & Neverdal, F. (2000) NE Atlantic continental rifting and volcanic margin formation. In: *Dynamics of the Norwegian Margin* (Ed. by Nottvedt) *Geol. Soc. London Spec. Publ.*, **167**, 295–326.

Talwani, M. & Eldholm, O. (1972) Continental margin off Norway; a geophysical study. *Geol. Soc. Am. Bull.*, **83**, 3575–3606.

Talwani, M. & Eldholm, O. (1977) Evolution of the Norwegian–Greenland Sea. *Geol. Soc. Am. Bull.*, **88**, 969–999.

Tsikalas, F., Faleide, J.I. & Eldholm, O. (2001) Lateral variations in tectono-magmatic style along the Lofoten–Vesteralen volcanic margin off Norway. *Marine Petrol. Geol.*, **18**, 807–832.

Tsikalas, F., Eldholm, O. & Faleide, J.I. (2002) Early Eocene sea floor spreading and continent-ocean boundary between Jan Mayen and Senja Frcature zones in the Norwegian–Greenland Sea. *Marine Geophys.l Res.*, **23**, 247–270.

Upton, B.G.J., Emeleus, C.H., Rex, D.C. & Thirlwall, M.F. (1995) Early tertiary magmatism in NE Greenland. *J. Geol. Soc. London*, **152**, 959–964.

White, R. & McKenzie, D. (1989) Magmatism at rift zones: the generation of volcanic continental margins and flood basalts. *J. Geophys. Res.*, **94**, 7685–7729.

White, R.S. & McKenzie, D. (1995) Mantle plumes and flood basalts. *J. Geophys. Res.*, **100**, 17543–17585.

Whitmarsh, R.B., Manatschal, G. & Minshull, T.A. (2001) Evolution of magma-poor continental margins from rifting to sea-floor spreading. *Nature*, **413**, 150–153.

Manuscript received 28 January 2004; Manuscript accepted: 13 April 2004.

